American Journal of Applied Science and Technology

VOLUME Vol.05 Issue 12 2025
PAGE NO. 175-179
DOI 10.37547/ajast/Volume05Issue12-31

Comprehensive Analysis Of Matrix-Type Nanostructured Columnar Composite Coatings Based On Anodic Aluminum And Tantalum Oxides

Shohruh Hudoykulov
Tashkent State Technical University, 100095, University str. 2, Tashkent, Uzbekistan

Sherzod Tashbulatov
Tashkent State Technical University, 100095, University str. 2, Tashkent, Uzbekistan

Laylo Xaytmetova
Tashkent State Technical University, 100095, University str. 2, Tashkent, Uzbekistan

Received: 26 October 2025; **Accepted:** 15 November 2025; **Published:** 21 December 2025

Abstract: Matrix-type nanostructured columnar composite coatings based on anodic aluminum oxide (Al_2O_3) and tantalum oxide (Ta_2O_5) represent a promising class of functional materials for advanced surface engineering applications. The anodization process enables the formation of ordered Nano porous and columnar structures with a high specific surface area, which can effectively serve as a matrix for composite oxide systems. In this study, the structural and morphological characteristics of anodic Al_2O_3–Ta_2O_5 composite coatings are analyzed, with particular emphasis on the formation of matrix-based nanostructured columnar architectures. The article analyzes the micromechanical properties of matrix nanostructures.

Keywords: Aluminum oxide, micromechanical properties, Al alloys, anodization process, tantalum oxide.

INTRODUCTION:

Of particular importance in the fields of modern materials science and surface Engineering is the issue of creating functional coatings. Nanostructured coatings in particular have high mechanical, electrical, and chemical properties and are widely used in the electronics, energy, medical, and aviation industries. In this context, coatings based on aluminium and tantalum oxides produced by the anodizing method are of great scientific and practical interest [1-6].

Anode aluminum oxide (Al_2O_3) and tantalum oxide (Ta_2O_5) are characterized by high dielectric impermeability, chemical stability, corrosion resistance, and heat tolerance properties. In particular, Matrix nanostructured columnar (porist) structures formed during anodizing greatly increase the functionality of the material.node aluminum oxide (Al_2O_3) and tantalum oxide (Ta_2O_5) are characterized by high dielectric impermeability, chemical stability, corrosion resistance, and heat tolerance properties [7-10]. In particular, Matrix nanostructured columnar (porist) structures formed during anodizing greatly increase the functionality of the material. Such structures have a high specific surface area and act as an effective matrix to create composite coatings.

In Matrix nanostructured columnar Composite coatings, electrical, optical and mechanical properties can be controlled by placing various functional components inside the oxide matrix. And the combined use of aluminum and tantalum oxides makes it possible to increase the reliability, dielectric properties and service life of the composite coating. Such coatings are particularly promising in capacitors, sensors, Microelectronics elements, and biomedical devices [11-13].

At the same time, an in-depth study of the processes of formation of Matrix nanostructured columnar Composite coatings of anode aluminum and tantalum oxides, determining the relationship between their morphology, structure and functional properties, remains an important scientific task. This article covers the results of research in this particular direction and analyzes the structural and practical properties of the obtained coatings [14].

Experimental Studies

Figure 1 presents electron microscopic images of AAO matrices. In these images, the pores were filled with columns by re-anodization in oxalic acid at applied voltages of 45 V and 450 V [15,16]. All images of the sample can be conventionally divided into approximately four regions: the upper layer of the anodic oxide ($h_{(up)}$), the outer ATO layer ($h_{(low)}$) consisting of nanoscale columns filling the AAO pores, the unanodized tantalum (Ta) film layer, and the silicon substrate.

The thickness-dependence plots correspond to $h_{(up)}$, $h_{(low)}$, and the total thickness of the formed dielectric film, where $h_{(tot)} = h_{(up)} + h_{(low)}$. As can be seen from Figure 1, metallic tantalum is polycrystalline and is covered with rod-shaped grains formed during magnetron sputtering of the films. The dark band observed at the interface between metallic Ta and AAO is most likely a dense barrier layer.

Oxide columns of different contrast emerge from the dark interfacial line, extend toward the AAO surface, and completely fill the pores. Both the interfacial band and the columns consist of oxide phases, within which a noticeable scattering of electrons is observed, making the columns clearly distinguishable from the AAO matrix. The average diameter of the columns (equivalent circular diameter) was determined to be approximately 50 nm, which is about 2.5 times larger than the average pore size of the corresponding AAO (~20 nm). The results illustrating the relationship between the dimensions of the columnar matrix-type nanostructures and the re-anodization voltages are presented. In addition, the ratio of the initial metal layer thickness required to form fully dense, pore-free structures has been determined.

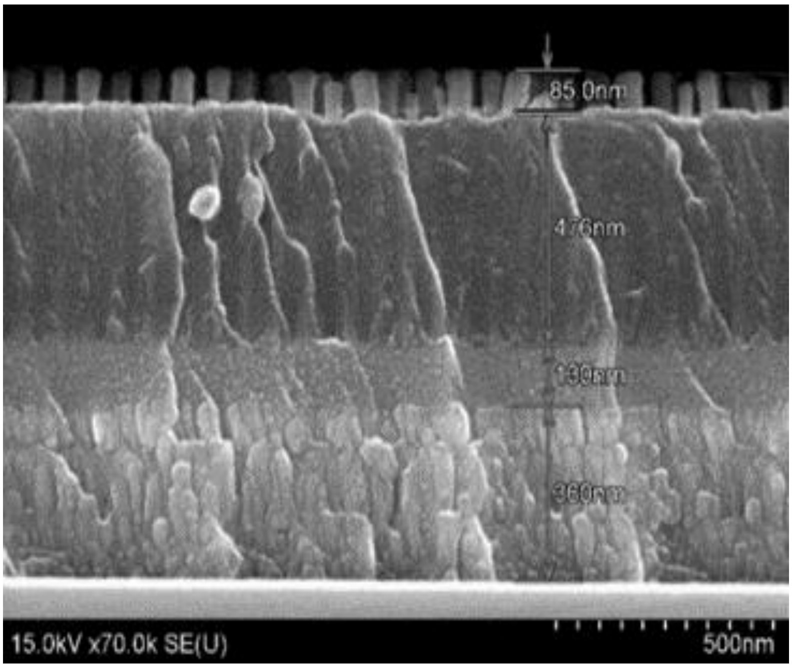

Figure 1. Image of a columnar matrix-type nanostructure formed as a result of anodization of a two-layer Al/Ta system in a 0.2 M oxalic acid solution followed by re-anodization in a 0.5 M boric acid solution.

RESULTS AND DISCUSSION

Figure 2 shows the dependence of the friction force, friction coefficient, and cantilever penetration depth on the applied load in the scratch testing apparatus. The experimental results demonstrate the high mechanical strength of the composite matrix–columnar anodic oxide films. At a maximum load of 50 mN, the penetration depth of a 2 µm diameter diamond indenter did not exceed 20% of the 1.5 µm film thickness after the first pass and 50% after the sixth pass.

A nonlinear dependence of the friction force, friction coefficient, and cantilever penetration depth on the applied load is observed, while the friction coefficient shows only a weak variation at loads up to 20 mN.

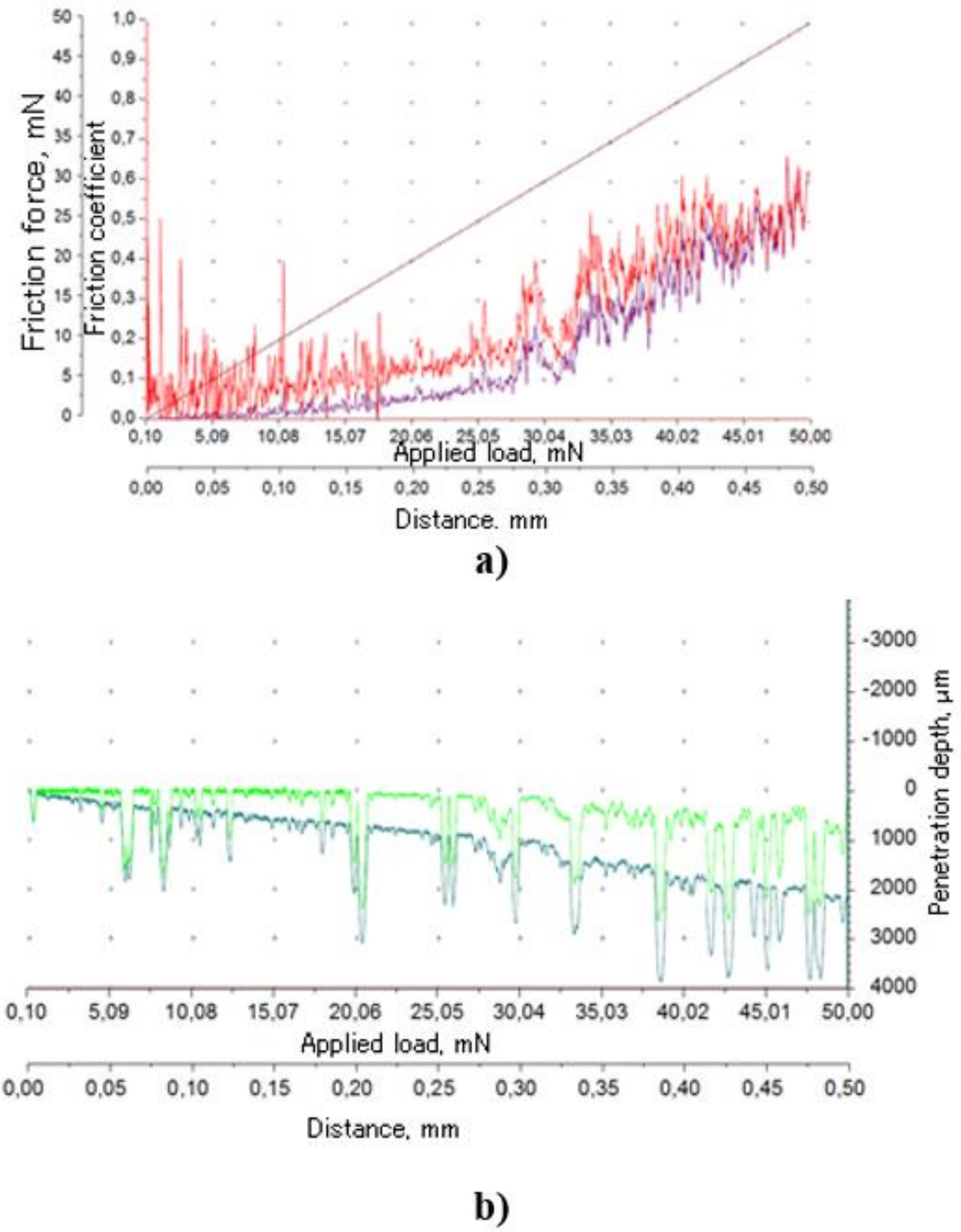

Figure 2. Dependence of the friction force and friction coefficient, as well as the cantilever penetration depth after the sixth pass, on the applied load. (a) Load dependence of the friction force and friction coefficient; (b) Load dependence of the cantilever penetration depth.

Nanoindentation was performed using Berkovich three-sided diamond indenters at maximum loads P_{max} = 10, 30, and 50 mN. The indentation process involved loading the indenter to P_{max} at a rate of 20 mN/min, holding the maximum load for 30 s, and then unloading. For each P_{max} value, five measurements were carried out on the test sample to determine the average values of microhardness and elastic modulus. Analysis of the nanoindentation load–displacement curves (Figure 3) was performed according to the Oliver–Pharr methodology. The average values of microhardness and elastic modulus are presented in Table 1

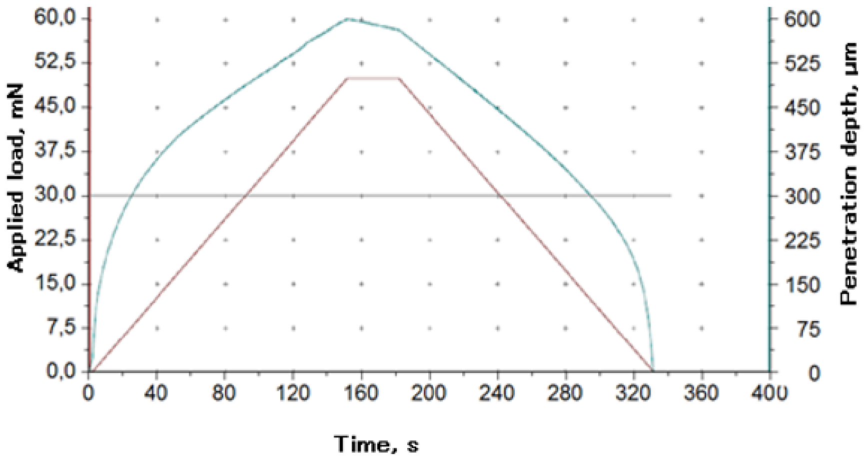

a)

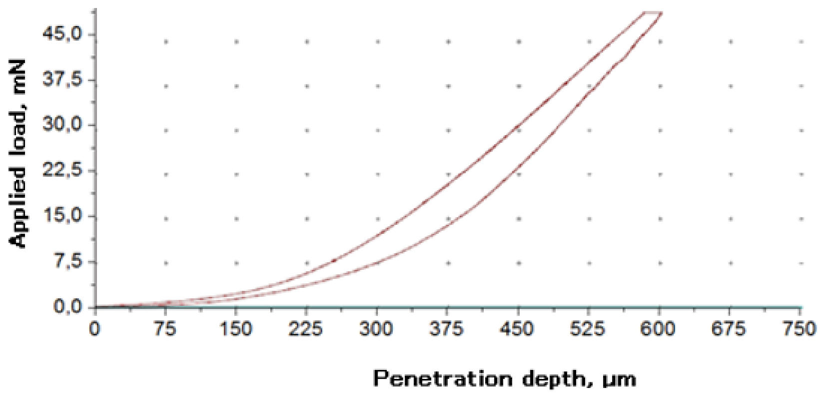

b)

Figure 3. Indentation kinetics and load–displacement (P–h) diagrams of the anodized Ta/Al system. (a) Indentation kinetics;(b) Load–displacement (P–h) diagram.

The obtained results on the micromechanical properties of the matrix-type nanostructures were compared with those of advanced Nano ceramic materials.

Table 1. Micro hardness (H) and elastic modulus (E□).

P_{max}	Depth, h	N, MPa	E_p, GPa
50 mN	610 nm	7056.2	93.5
30 mN	460 nm	4983.2	84.9
10 mN	330 nm	4630.7	87.0

CONCLUSION

The experimental results presented above indicate that the average values of the elastic modulus and microhardness remain nearly unchanged at applied loads of 10 and 30 mN, whereas a significant increase is observed under an applied load of 50 mN.

REFERENCES

1. Drevet, R., Souček, P., Mareš, P., Ondračka, P., Dubau, M., Kolonits, T., Czigány, Z., Balázsi, K., & Vašina, P. (2024). Aluminum tantalum oxide thin films deposited at low temperature by pulsed direct current reactive magnetron sputtering for

dielectric applications. Vacuum, 221. https://doi.org/10.1016/j.vacuum.2023.112881

2. Nickel, M. R., Melligan, G., McMullen, T. P. W., & Burrell, R. E. (2019). The effect of chemical additives in phosphoric acid anodization of aluminum-tantalum thin films. Thin Solid Films, 685. https://doi.org/10.1016/j.tsf.2019.06.033
3. Turakhodjaev, N. D., Tursunbaev, S. A., Odilov, F. U., Zokirov, R. S., & Kuchkarova, M. Kh. (2020). Vliyanie uslovii legirovaniya na svoistva belykh chugunov [Influence of alloying conditions on the properties of white cast irons]. In Tekhnika i tekhnologii mashinostroeniya (pp. 63–68).
4. Okayasu, M., Takeuchi, S., & Shiraishi, T. (2013). Corrosion and mechanical properties of cast aluminium alloys. International Journal of Cast Metals Research, 26(6), 319–329. https://doi.org/10.1179/1743133613Y.0000000067
5. Umarov, T. U., Tursunbaev, S. A., & Mardonov, U. T. (2018). Novye tekhnologicheskie vozmozhnosti povysheniya ekspluatatsionnoi nadezhnosti instrumentov dlya obrabotki kompozitsionnykh materialov [New technological possibilities for improving the operational reliability of tools for machining composite materials]. In Tekhnika i tekhnologii mashinostroeniya (pp. 70–74).
6. Hirsch, J., Skrotzki, B., & Gottstein, G. (Eds.). (2008). Aluminium alloys: The physical and mechanical properties (Vol. 1). Wiley-VCH.
7. Tursunbaev, S., Umarova, D., Kuchkorova, M., & Baydullaev, A. (2022). Study of machining accuracy in ultrasonic elliptical vibration cutting of alloyed iron alloy carbon with germanium. Journal of Physics: Conference Series, 2176(1), 012053. https://doi.org/10.1088/1742-6596/2176/1/012053
8. Sarvar, T., Nodir, T., Mardonov, U., Saydumarov, B., Kulmuradov, D., & Boltaeva, M. (2024). Effects of germanium (Ge) on hardness and microstructure of Al–Mg, Al–Cu, and Al–Mn system alloys. International Journal of Mechatronics and Applied Mechanics, (16), 179–184.
9. Drevet, R., Souček, P., Mareš, P., Ondračka, P., Fekete, M., Dubau, M., & Vašina, P. (2025). Influence of oxygen flow on the structure, chemical composition, and dielectric strength of AlxTayOz thin films deposited by pulsed-DC reactive magnetron sputtering. Surface and Coatings Technology, 498. https://doi.org/10.1016/j.surfcoat.2025.131865
10. Tursunbaev, S., Turakhodjaev, N., Turakhujaeva, S., Ozodova, S., Hudoykulov, S., & Turakhujaeva, A. (2022). Reduction of gas porosity when alloying A000 grade aluminum with lithium fluoride. IOP Conference Series: Earth and Environmental Science, 1076(1), 012076. https://doi.org/10.1088/1755-1315/1076/1/012076
11. Gao, Y. X., Yi, J. Z., Lee, P. D., & Lindley, T. C. (2004). The effect of porosity on the fatigue life of cast aluminium–silicon alloys. Fatigue & Fracture of Engineering Materials & Structures, 27(7), 559–570. https://doi.org/10.1111/j.1460-2695.2004.00763.x
12. Roven, H. J., Nesbø, H., Werenskiold, J. C., & Seibert, T. (2005). Mechanical properties of aluminium alloys processed by severe plastic deformation: Comparison of different alloy systems and possible product areas. Materials Science and Engineering: A, 410–411, 426–429. https://doi.org/10.1016/j.msea.2005.08.153
13. Skejić, D., Dokšanović, T., Čudina, I., & Mazzolani, F. M. (2021). The basis for reliability-based mechanical properties of structural aluminium alloys. Applied Sciences, 11(10), 4485. https://doi.org/10.3390/app11104485
14. Anusionwu, B. C., Adebayo, G. A., & Madu, C. A. (2009). Thermodynamics and surface properties of liquid Al–Ga and Al–Ge alloys. Applied Physics A, 97(3), 533–541. https://doi.org/10.1007/s00339-009-5334-4
15. Miura, K., & Omi, K. (2024). Near-infrared light emission from aluminum-doped tantalum-oxide thin films prepared using a simple co-sputtering method. Results in Physics, 57. https://doi.org/10.1016/j.rinp.2024.107389
16. Hu, B. Q., Wang, X. M., Zhou, T., Zhao, Z. Y., Wu, X., & Chen, X. L. (2001). Transmittance and refractive index of the lanthanum strontium aluminium tantalum oxide crystal. Chinese Physics Letters, 18(2). https://doi.org/10.1088/0256-307X/18/2/342